JOURNAL OF VIROLOGY, Nov. 2010, p. 11718–11728 Vol. 84, No. 22
0022-538X/10/$12.00 doi:10.1128/JVI.00798-10

Cytopathogenesis of Sendai Virus in Well-Differentiated Primary Pediatric Bronchial Epithelial Cells▽†

Rémi Villenave,[1] Olivier Touzelet,[1] Surendran Thavagnanam,[1] Severine Sarlang,[1] Jeremy Parker,[1] Grzegorz Skibinski,[1] Liam G. Heaney,[1] James P. McKaigue,[2] Peter V. Coyle,[3] Michael D. Shields,[1,2] and Ultan F. Power[1]*

Centre for Infection & Immunity, School of Medicine, Dentistry & Biomedical Sciences, Queens University Belfast, Belfast, Northern Ireland[1]; the Royal Belfast Hospital for Sick Children, Belfast, Northern Ireland[2]; and the Regional Virus Laboratory, Belfast Trust, Belfast, Northern Ireland[3]

Received 15 April 2010/Accepted 24 August 2010

Sendai virus (SeV) is a murine respiratory virus of considerable interest as a gene therapy or vaccine vector, as it is considered nonpathogenic in humans. However, little is known about its interaction with the human respiratory tract. To address this, we developed a model of respiratory virus infection based on well-differentiated primary pediatric bronchial epithelial cells (WD-PBECs). These physiologically authentic cultures are comprised of polarized pseudostratified multilayered epithelium containing ciliated, goblet, and basal cells and intact tight junctions. To facilitate our studies, we rescued a replication-competent recombinant SeV expressing enhanced green fluorescent protein (rSeV/eGFP). rSeV/eGFP infected WD-PBECs efficiently and progressively and was restricted to ciliated and nonciliated cells, not goblet cells, on the apical surface. Considerable cytopathology was evident in the rSeV/eGFP-infected cultures postinfection. This manifested itself by ciliostasis, cell sloughing, apoptosis, and extensive degeneration of WD-PBEC cultures. Syncytia were also evident, along with significant basolateral secretion of proinflammatory chemokines, including IP-10, RANTES, tumor necrosis factor (TNF)-related apoptosis-inducing ligand (TRAIL), interleukin 6 (IL-6), and IL-8. Such deleterious responses are difficult to reconcile with a lack of pathogenesis in humans and suggest that caution may be required in exploiting replication-competent SeV as a vaccine vector. Alternatively, such robust responses might constitute appropriate normal host responses to viral infection and be a prerequisite for the induction of efficient immune responses.

Sendai virus (SeV) is a nonsegmented negative-strand RNA virus of the *Paramyxoviridae* family. Recombinant SeV (rSeV) has been extensively studied as a vector for vaccines, cancer immunotherapy, and gene therapy (14, 22, 34, 41, 43). SeV is virulent in rodents, but despite extensive antigenic and genetic similarity to human parainfluenza virus type 1 (hPIV1), it is not known to cause disease in humans (33). Interest in rSeV as a vector is exemplified by the fact that (i) its genome can easily be manipulated to stably express heterologous genes (9), (ii) it does not undergo homologous recombination, (iii) cell transduction is independent of the cell cycle, (iv) there is no DNA phase during replication and hence no possibility of cell transformation, and (v) its cell or tissue tropisms and replication competency may be modulated by reverse genetics and appropriate rescue systems (5, 8).

Much of the research on rSeV as a vector involves monolayer cells and animal models and employs both replication-competent and transmission-incompetent viruses. In view of its respiratory tract tropism, particular attention was paid to its use as a gene therapy vector for lung diseases such as cystic fibrosis (CF) (2, 13, 14, 43). Indeed, early studies demonstrated its capacity to efficiently overcome a series of extra- and intracellular barriers in the respiratory tract, such as the glycocalyx, mucus layer, mucociliary clearance, and cell membranes (13, 14, 43). However, *in vivo* studies demonstrated that rSeV-mediated gene transduction was transient (lasting ~7 days) and that repeated administration was inefficient (16). The reasons for this transient transduction remain unclear.

In contrast, the capacity to efficiently and transiently transduce host cells is of considerable interest from a vaccine vector viewpoint. Indeed, promising rSeV-vectored vaccine candidates have been described for other respiratory viruses, such as respiratory syncytial virus (RSV), hPIV1, hPIV2, hPIV3, and systemic viruses, such as HIV-1 (22, 40, 44). Despite its considerable promise as a viral vector, little is known about how rSeV interacts with human airway epithelial cells (HAE).

To address this, we established an *ex vivo*/*in vitro* model of respiratory virus infection based on well-differentiated primary pediatric bronchial epithelial cells (WD-PBECs) in air-liquid interface (ALI) cultures. The pediatric origin of the primary bronchial cells allowed us to investigate SeV-host interactions in a pediatric context. The need for CF gene therapy or respiratory virus vaccines for infants or children emphasizes the relevance of this *ex vivo*/*in vitro* pediatric model. Using rSeV expressing enhanced GFP (rSeV/eGFP), we comprehensively investigated the consequences of SeV infection in these cultures, including the types of cells infected, virus growth kinetics, cytopathic effects (CPE), and inflammatory responses. Our

* Corresponding author. Mailing address: Centre of Infection & Immunity, Scholl of Medicine, Dentistry & Biomedical Sciences, Queen's University Belfast, Medical Biology Centre, 97 Lisburn Road, Belfast BT9 7BL, Northern Ireland. Phone: 44 (0)28 9097 2285. Fax: 44 (0)28 9097 2695. E-mail: u.power@qub.ac.uk.

† Supplemental material for this article may be found at http://jvi.asm.org/.

▽ Published ahead of print on 1 September 2010.

TABLE 1. Cell counts and TEER measurements of WD-PBEC cultures before infection

Donor	Cell count 21 days after ALI	TEER (mean ± SEM)	No. of inserts excluded/total
1	1×10^6	537.6 ± 11.2	8/24
2	1.2×10^6	378 ± 6.2	3/12
3	1.1×10^6	761.6 ± 28	0/24
4	1.02×10^6	692.7 ± 82.3	0/8
5	4.1×10^5	688.8 ± 5.6	0/24

data provided novel insights into the interaction of SeV with pediatric airway epithelium and the limitations and/or advantages of its use as a vector.

MATERIALS AND METHODS

Cell line and viruses. LLC-MK2 cells were cultured as previously described (38). rSeV/eGFP was rescued from an infectious SeV clone containing the *eGFP* gene inserted between the SeV *N* and *P* genes, as previously described (38). Briefly, *eGFP* was amplified using *Pfu* Turbo DNA polymerase (Stratagene) and the *eGFP*-specific primers ATTA**ACGCGTA**TCCACCGGTCGCCACCATGGT GAGC (forward) and TACT**ACGCGT**TTTACTTGTACAGCTCGTCCAT GCCG (reverse), which contain MluI sites (in bold), and cloned into the unique MluI site of pSeV FL4 N3′ AatII-MluI.

rSeV/eGFP stocks were grown in embryonated chicken eggs as previously described (38). Titration of rSeV/eGFP, either in viral stocks or experimental samples, was performed in LLC-MK2 cells as previously described (38), except that infections were undertaken in the absence of acetylated trypsin. This limits SeV replication to a single round of infection. After 48 h of incubation at 37°C in 5% CO_2, the numbers of fluorescent cells were counted in appropriate dilutions under a UV microscope (Nikon TE2000), and titers were calculated as numbers of fluorescent focus units (FFU)/ml.

WD-PBECs. Primary pediatric bronchial epithelial cells (PBECs) were obtained by bronchial brushings from healthy children undergoing elective surgery, as described before (12). All cell samples were confirmed to be negative for a panel of 12 respiratory viruses using a multiplex virus reverse transcriptase (RT) PCR strip, as previously described (11), before inclusion in the study. They were then used to generate well-differentiated PBECs (WD-PBECs), as recently described (27). Briefly, the cells were seeded in collagen-coated (Purecol; Inamed, United Kingdom) 10-cm^2 flasks (Nunc, United Kingdom) using airway epithelial cell basal medium (catalog no. C-21260) supplemented with supplement pack/airway epithelial growth medium (catalog no. C-39160) (Promocell, Germany) at 37°C in 5% CO_2 until almost confluent. They were then passaged into a collagen-coated 75-cm^2 flask and expanded at 37°C in 5% CO_2. Upon reaching 80% confluence, the cells were trypsinized (0.5% trypsin-EDTA; GIBCO, United Kingdom) and seeded onto collagen-coated, semipermeable membrane supports (Transwell-Col, 12-mm diameter, 0.4-μm pore size; Corning-Costar, Corning, NY) at 10^5 cells/well. When confluence was reached, the apical medium was removed and the ALI established to trigger differentiation. Cells were maintained at the ALI for 21 days, with the basolateral medium changed every second day and the apical side rinsed with phosphate-buffered saline (PBS) every week to remove excess mucus production. The transepithelial electric resistance (TEER) was determined for each transwell using EVOM^2 and an Endohm chamber (World Precision Instruments). Cultures with TEERs of ≥300 Ω · cm^2 were retained for experimentation.

Infection of WD-PBECs. All infections were undertaken in WD-PBEC cultures 21 days after initiation of ALI culture. rSeV/eGFP stocks were thawed rapidly and diluted in culture medium to prepare a multiplicity of infection (MOI) of ~4 in 800 μl. MOIs were calculated based on cell counts following trypsinization of a single transwell culture for each donor (the cell count and TEER [mean ± standard error of the mean }SEM{] for each donor are provided in Table 1). Inocula were added to the apical surface, and cultures were incubated for 2 h at 37°C in 5% CO_2. Control wells received 800 μl of culture medium. After 2 h, the apical surface was rinsed 6 times with 500 μl warm PBS. After the final wash and every 24 h thereafter, the apical surface was rinsed and the basal medium harvested to determine virus growth kinetics and cytokine/chemokine responses, respectively. Apical rinses were obtained by adding 500 μl PBS to the apical surface for 10 min at 37°C, harvesting the rinse, and snap-freezing and storing it in liquid nitrogen. The basal medium was stored at −80°C and replaced with fresh culture medium. Infected and control cultures were monitored daily by light and UV microscopy (Nikon Eclipse TE-2000 U; Nikon, United Kingdom). GFP quantification of infected cultures was performed using ImageJ software (http://rsbweb.nih.gov/ij/). Briefly, representative fields of infected cultures were photographed every 24 h by UV microscopy and converted in 8 bits, and mean gray pixel values of the fields were measured using ImageJ software.

Cytospins. To determine the consequence of rSeV/eGFP infection on epithelial cell sloughing, apical surfaces of dedicated infected and control WD-PBEC cultures were rinsed every 24 h as described above and 250 μl of the apical washings was added to each of 2 cytospin sample chambers (Shandon). The chambers were centrifuged at 1,000 × *g* for 2 min in a Cytospin 3 centrifuge (Shandon). Following removal of the filters and chambers, the cells were air dried for 1 h at room temperature, fixed with 100% ice-cold acetone for 15 min, rinsed with PBS, and either stained directly or stored at −20°C until used. Quantification of nuclei was performed using a UV microscope (Nikon Eclipse TE-2000 U; Nikon, United Kingdom) following DAPI (4′,6-diamino-2-phenylindole) staining.

Immunofluorescence assays. Both the apical and basolateral compartments of the WD-PBEC cultures were rinsed 3 times with 500 μl PBS. Paraformaldehyde (4%, vol/vol) was added to the apical (500 μl) and basal (1.5 ml) compartments for 20 min, and the PBS washings were repeated. Cultures were stored in 70% ethanol at 4°C until used. For immunofluorescent staining, the ethanol was removed and the cells were rinsed 3 times with 500 μl PBS, permeabilized with PBS plus 0.2% Triton X-100 (vol/vol) (Sigma) for 2 h at room temperature, and blocked with 10% nonimmune normal goat serum (Zymed) for 30 min. The cultures were stained for ciliated cells (anti-β-tubulin clone Tub 2.1, 1:100 [Sigma]) or goblet cells (anti-Muc5AC clone 45M1, 1:200 [Abcam]). Briefly, 200 μl primary antibody was added to the apical surface for 1 h at 37°C, the cultures were washed 3 times with 500 μl PBS for 15 min at room temperature, 200 μl Alexa 568-conjugated secondary goat anti-mouse IgG (1:500; Molecular Probes, United Kingdom) was added for 1 h at 37°C, and the washings were repeated. Inserts were mounted on microscopy slides using DAPI mounting medium (Vectashield; Vector Laboratories). Fluorescence was detected by confocal laser scanning microscopy (TCS SP5; Leica, Germany).

TUNEL assay. Apoptosis was detected with the terminal deoxynucleotidyl-transferase-mediated dUTP-biotin nick end labeling (TUNEL) system, as described by the manufacturer (Roche).

Transmission electron microscopy. WD-PBECs were fixed with 1% osmium tetroxide for 1 h, followed by dehydration in a series of graded ethanols. Cultures were infiltrated with Epon resin and 80-nm sections cut. Sections were then mounted on copper grids and stained with 5% uranyl acetate-2.6% lead citrate and observed under a Philips CM 100 transmission electron microscope.

Cytokine/chemokine concentration determination. Basolateral samples were thawed and analyzed for a panel of cytokine/chemokine concentrations using custom Bio-Plex assay kits (Bio-Rad, United Kingdom). The panel included RANTES (CCL5), IP-10 (CXCL10), interleukin 6 (IL-6), IL-8 (CXCL8), tumor necrosis factor (TNF)-related apoptosis-inducing ligand (TRAIL), and vascular endothelial growth factor (VEGF). Analyte concentrations were determined according the manufacturer's instructions, using a Bio-Plex 200 system (Bio-Rad, United Kingdom).

Statistical analyses. All data were analyzed with a paired *t* test using GraphPad Prism 5.0. Values are presented as means ± standard errors. A P value of <0.05 was considered statistically significant.

Ethics. This study was approved by the Office for Research Ethics Committees, Northern Ireland. Written informed consent and assent were obtained from all parents and children, where appropriate, prior to bronchial brushings.

RESULTS

Structure and integrity of the WD-PBEC model. An *ex vivo*/*in vitro* model of well-differentiated pseudostratified bronchial epithelium based on pediatric epithelial cells derived from bronchial brushings was exploited for the current studies (27). Following 21 days of ALI culture, WD-PBECs were found to have an extensive coverage of beating cilia, as evidenced by light microscopy, and copious production of mucus (data not shown). Robust transepithelial electric resistances (TEERs) of ≥300 Ω · cm^2 were also evident for the vast majority of transwells (data not shown). A minimum TEER value

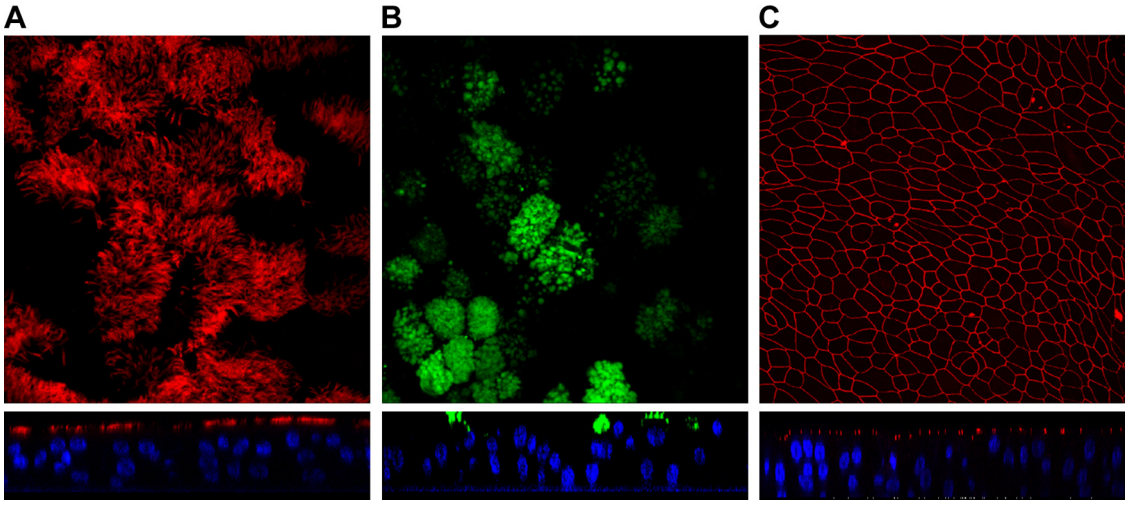

FIG. 1. Structure and integrity of the WD-PBEC model. WD-PBECs were grown at the air-liquid interface for 21 days, washed, and fixed. WD-PBECs were stained with a mouse anti-β-tubulin MAb (specific for ciliated cells) and a goat anti-mouse secondary antibody coupled with Alexa 568 (red) (A), with a mouse anti-Muc5AC MAb (specific for goblet cells) and a goat anti-mouse secondary antibody coupled with Alexa 488 (green) (B), or with a mouse anti-ZO-1 MAb (specific for tight junctions) and a goat anti-rabbit secondary antibody coupled with Alexa 568 (red) (C). Slides were observed under a confocal microscope. *En face* views and confocal orthogonal sections are shown in the upper and lower panels, respectively. Original magnifications were ×184 (A), ×160 (B), and ×40 (C). These photos are representative of cultures from 5 individual donors.

of 300 $\Omega \cdot cm^2$ was set as a prerequisite for use of transwells in subsequent experiments. As expected, confocal microscopy confirmed the presence of ciliated and goblet cells on the apical surfaces of the cultures, well-established tight junctions, and culture thicknesses of 3 to 6 cell layers (Fig. 1A, B, and C).

rSeV/eGFP infects and replicates efficiently in WD-PBECs. To determine the capacity of rSeV/eGFP to infect WD-PBECs, cultures ($n = 5$) were inoculated at an MOI of ~4. Typical rSeV/eGFP infections of WD-PBECs are represented in Fig. 2A, and GFP quantification is presented in Fig. 2B. By 24 h postinfection (hpi), there was clear evidence of infection with rSeV/eGFP, as determined by eGFP expression. The intensity of eGFP expression progressed significantly between 24 and 48 hpi and peaked at around 72 hpi. Based on eGFP expression, the infection spread to virtually all parts of the culture. Progression of infection seemed to be directed and followed the stream of mucus created by the synchronized beat of the cilia. Evidence for the stream of mucus is shown in movie S1 in the supplemental material. At later time points, there was clear evidence of considerable cytopathic effects (CPE), which manifested themselves in the form of holes in the cultures. This coincided with a diminishing epithelium barrier integrity, as quantified over time by measuring the TEERs of infected versus uninfected cultures (Fig. 2C).

The growth curve data (Fig. 3) demonstrated that infectious rSeV/eGFP was released from the apical surfaces of WD-PBECs from an early time point. Large quantities of virus were released by 24 hpi, while peak titers were evident between 48 and 72 hpi. Thereafter, titers diminished slightly until the end of the experiment, but the rSeV/eGFP-infected WD-PBEC cultures remained highly productive for the duration of the experiments. Interestingly, no virus was detected in the basolateral compartment of the transwells at any time point. This was not due to an inability of the virus to traverse the porous collagen-coated transwell membrane, as evidenced by the ability of rSeV/eGFP to cross these membranes in the absence of WD-PBEC cultures (data not shown). These data indicate that rSeV/eGFP infection and spread are restricted to the apical surfaces of the WD-PBEC cultures.

rSeV/eGFP infects apical ciliated and nonciliated epithelial cells but not goblet cells. To confirm the location of rSeV/eGFP infection within the WD-PBEC cultures and the types of cells involved, WD-PBECs ($n = 5$) were infected with rSeV/eGFP (MOI ≈ 4) and fixed with 4% paraformaldehyde 48 hpi. The cultures were stained with phycoerythrin-conjugated anti-β-tubulin (cilium specific) or anti-Muc5AC (goblet cell specific) monoclonal antibodies (MAbs). Orthogonal and *en face* confocal microscopy observations revealed that rSeV/eGFP infection was restricted to the apical surface (Fig. 4A). Furthermore, at 48 hpi, an average of 88% of ciliated epithelial cells were infected (Fig. 4B). However, not all eGFP-positive cells were ciliated, with up to 6% of infected cells being nonciliated. Interestingly, *en face* and confocal orthogonal section observations of the infected cultures also revealed the presence of eGFP within the cilia (Fig. 4C). In contrast, there was no evidence of infection of goblet cells (Fig. 4D).

rSeV/eGFP induces substantial CPE in WD-PBECs. rSeV/eGFP- and mock-infected WD-PBEC cultures were monitored for GFP fluorescence and CPE. Light microscopy and UV microscopy were undertaken every 24 h following infection. The typical progression of rSeV/eGFP-induced CPE is shown in Fig. 5A. At 144 hpi, holes were evident in the cultures, unlike in uninfected controls, which remained intact. The extent and frequency of the holes progressed over the following days, indicative of considerable destruction of the infected epithelial cultures. Moreover, orthogonal sections following confocal microscopy of rSeV/eGFP-infected WD-PBECs revealed a tendency toward fewer cell layers at 144 hpi (1 to 2 layers) than in mock-infected cultures (3 to 5 layers) (Fig. 5B).

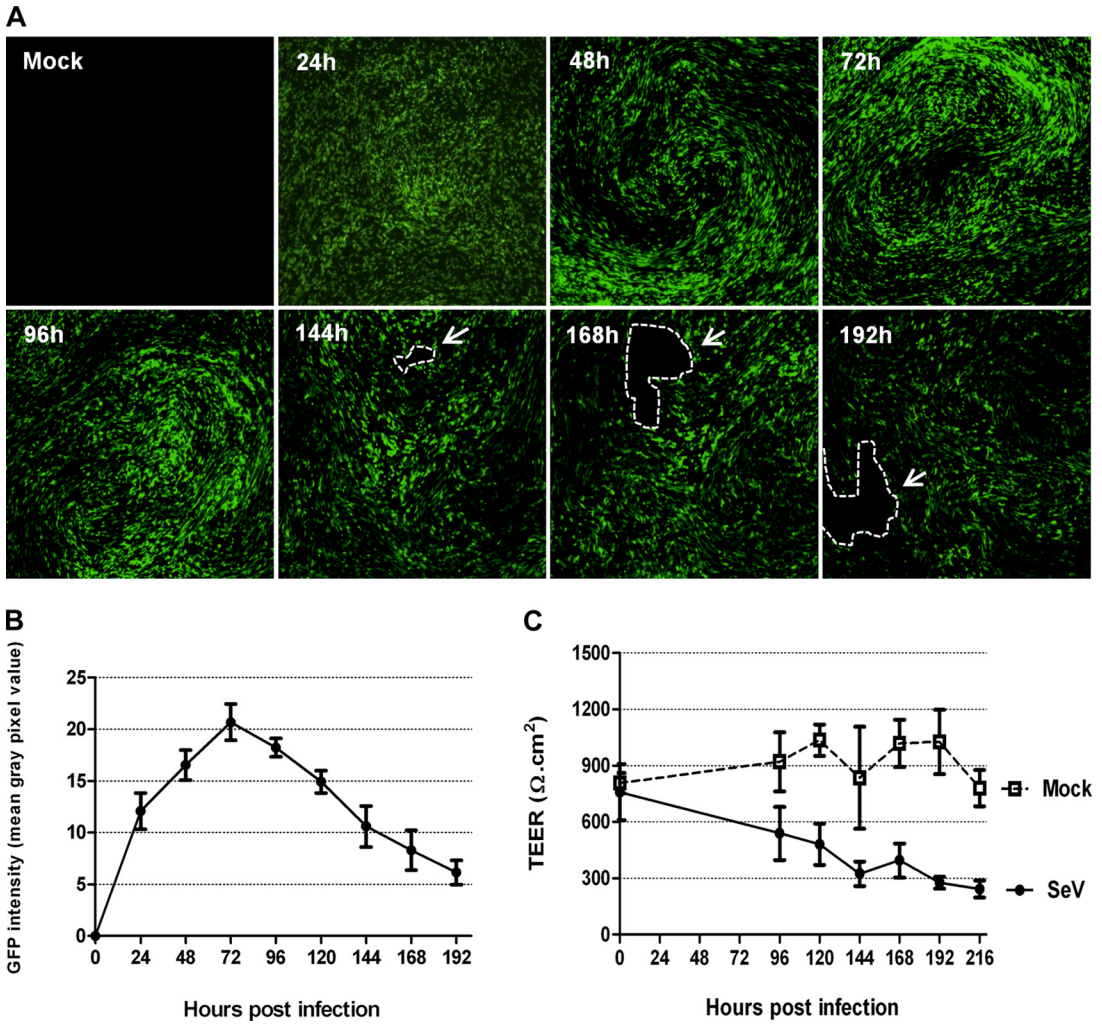

FIG. 2. Time course of rSeV/eGFP infection on WD-PBECs. The apical surfaces of WD-PBEC cultures were infected with rSeV/eGFP (MOI = 4), and eGFP expression was monitored by UV fluorescence microscopy every 24 h thereafter for 192 h as an indication of virus spread over time (A). White arrows and dashed lines indicate holes in the infected cultures. Original magnification, ×4. These photos are representative of cultures from 5 individual donors. GFP intensity over time was quantified by measuring the mean gray pixel values of representative fields using ImageJ software (n = 3 donors) (B). TEER was measured every 24 h following rSeV/eGFP or mock infection of WD-PBEC cultures (C). Data represent mean TEER values ± SEM (n = 3).

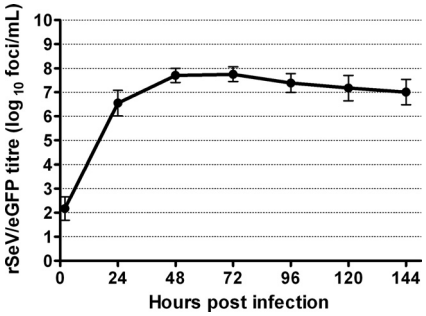

FIG. 3. Growth curve of SeV/eGFP in WD-PBECs. WD-PBEC cultures from five individual donors were infected in duplicate with rSeV/eGFP (MOI = 4) for 2 h and washed with PBS. Virus released to the apical surface was harvested at 2, 24, 48, 72, 96, 120, and 144 hpi, as described in Materials and Methods. Virus titers in apical washes were determined using LLC-MK2 cells in the absence of acetylated trypsin and are expressed as $\log_{10}$ fluorescent focus units/ml. Each point corresponds to the mean of results for 5 different donors. Data represent mean titers ± standard deviations.

Interestingly, although not measured, we also observed clear visual evidence of ciliostasis by 96 hpi (data not shown).

Cytospins were also performed every 24 hpi on apical rinses to determine the relative sloughing of apical cells in rSeV/eGFP-infected versus mock-infected WD-PBEC cultures. Representative and quantified data from all time points examined are shown in Fig. 5C and D, respectively. Nuclei were stained with DAPI. As expected, apical washes of infected WD-PBECs contained much more cell debris and damaged nuclei than mock-infected cultures.

Syncytium formation was clearly evident in rSeV/eGFP-infected WD-PBECs (Fig. 6), a novel observation. Syncytia are typical cytopathic characteristics of SeV infection in monolayer cells (31), resulting from membrane fusion between infected and neighboring cells. Two types of multinucleated syncytia were evident. In the first type, nuclei clustered in the center of the syncytium (Fig. 6A), whereas in the second type, nuclei

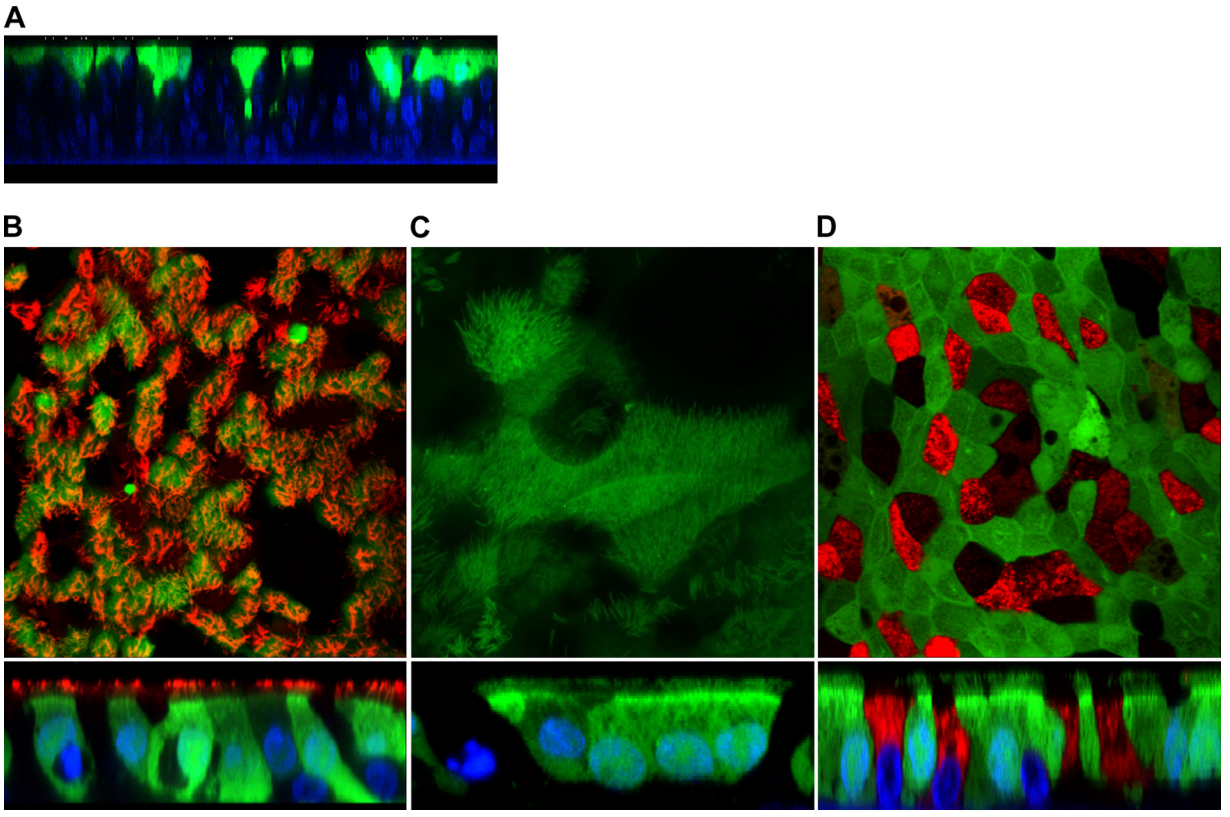

FIG. 4. rSeV/eGFP infects primarily ciliated cells and not goblet cells. WD-PBECs were infected with rSeV/eGFP (MOI = 4) for 2 h and washed with PBS. *En face* and confocal orthogonal sections of rSeV/eGFP-infected cultures were taken at 48 hpi. (A) A representative confocal orthogonal section of rSeV/eGFP-infected cultures at 48 hpi is presented (blue, DAPI-stained nuclei; green, eGFP). (B) WD-PBECs were fixed and stained with phycoerythrin-conjugated anti-β-tubulin MAb (red) (specific for ciliated cells) and examined under confocal microscopy at a ×90 magnification. (C) WD-PBECs were fixed, and cilia were examined under confocal microscopy at a ×126 magnification (green, eGFP). rSeV/eGFP infection is restricted to the apical layer (blue, DAPI-stained nuclei; green, eGFP). (D) Alternatively, fixed cultures were stained with a mouse anti-Muc5AC MAb followed by an Alexa 568-coupled goat anti-mouse secondary antibody (red) and observed at a ×90 magnification.

were organized at the perimeter of the syncytium (Fig. 6B). Interestingly, the confocal data suggested that the second type is the result of vacuole formation in the center of the syncytium itself, with the nuclei organizing themselves around the periphery of the vacuole (Fig. 6C). Indeed, this is corroborated by electron microscopy data, in which large vacuoles are evident only in rSeV/eGFP-infected WD-PBECs (Fig. 6D). The possibility remains that these two syncytium types represent different stages of development of the syncytium following infection.

Apoptosis is triggered by rSeV/eGFP infection. The CPE and cytospin data indicated that considerable cell death occurred following rSeV/eGFP infection. A number of lines of evidence suggest that apoptosis was responsible, at least in part, for this cell death. First, characteristic apoptosis-associated cell blebbing was detected as early as 48 hpi (Fig. 7A). Second, chromatin condensation (karyopyknosis) and nuclear fragmentation (karyorrhexis) were also clearly evident following infection (Fig. 7B). In contrast, nuclear integrity was conserved in mock-infected cells. Finally, TUNEL assays performed on infected and mock-infected WD-PBEC cultures fixed at 8, 24, 48, and 144 hpi confirmed the presence of apoptotic cells on the apical surface from 24 h following rSeV/eGFP infection. In contrast, mock-infected cultures were negative for TUNEL staining (Fig. 7C).

rSeV/eGFP induces substantial secretion of proinflammatory cytokines and chemokines. To further characterize the interaction of rSeV/eGFP with WD-PBECs, we determined the concentrations of a range of cytokines/chemokines in the basolateral medium at 24 and 120 hpi compared with those in mock-infected controls. These included IL-6, IL-8, TRAIL, IP-10, VEGF, and RANTES (Fig. 8). As the basolateral medium was replaced every day, the chemokine/cytokine concentrations reported represent secretions over the 24-h period preceding the sample time point, rather than cumulative secretions over the entire experimental period. Of the analytes tested, only IP-10 and RANTES were significantly elevated at 24 hpi compared to their levels in the negative controls ($P < 0.001$ and $P < 0.05$, respectively). By 120 hpi, the concentrations of IP-10 and RANTES were further increased ($P < 0.001$ and $P < 0.05$, respectively) and TRAIL and IL-6 levels were also significantly elevated ($P < 0.05$). There was a trend toward increased IL-8 by 120 hpi, although this did not reach significance. Interestingly, IL-8 concentrations were very high in all samples. Absolute concentrations of IP-10 were very high in the basolateral medium derived from rSeV/eGFP-infected cul-

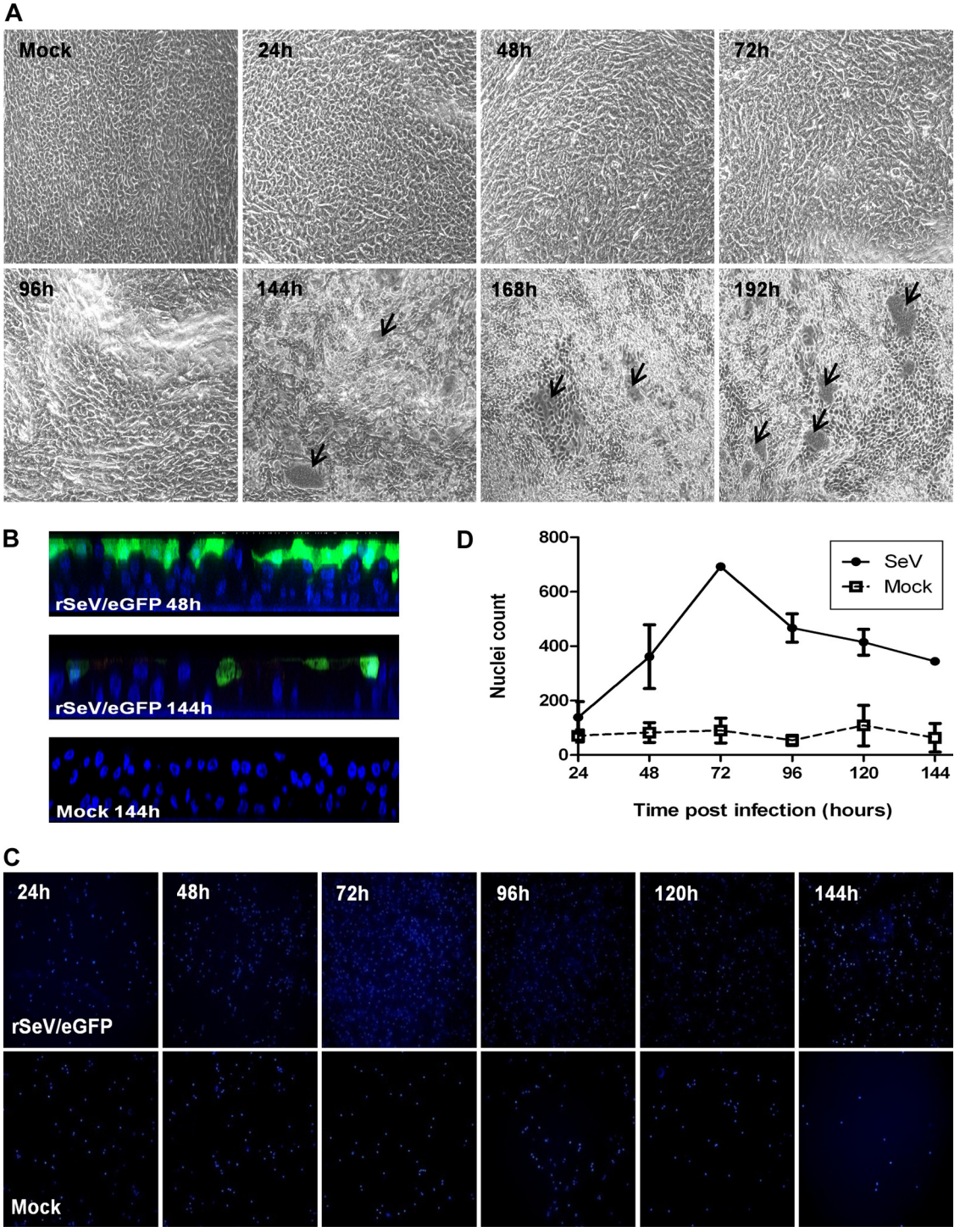

FIG. 5. Cytopathic effects in rSeV/eGFP-infected cultures. WD-PBECs were infected for 2 h with rSeV/eGFP (MOI = 4) and washed with PBS. (A) *En face* phase-contrast microphotographs were taken every 24 h following infection. Representative images are shown for mock-infected cultures and every 24 h following rSeV/eGFP infection. The image of the mock-infected culture is representative of all the time points. Original magnification, ×10. These images are representative of cultures from 5 individual donors. (B) Confocal orthogonal sections of rSeV/eGFP-infected cultures at 48 and 144 hpi. Nuclei were stained with DAPI. Original magnification, ×40. (C) Representative cytospins of apical rinses from rSeV/eGFP-infected (upper panels) and mock-infected (lower panels) cultures at 24, 48, 72, 96, 120, and 144 hpi. Cells were stained with DAPI. The fields are representatives of all slides. Original magnification, ×10. (D) Quantification of nuclei in apical rinses at different times postinfection ($n = 3$). Data represent mean values ± standard deviations.

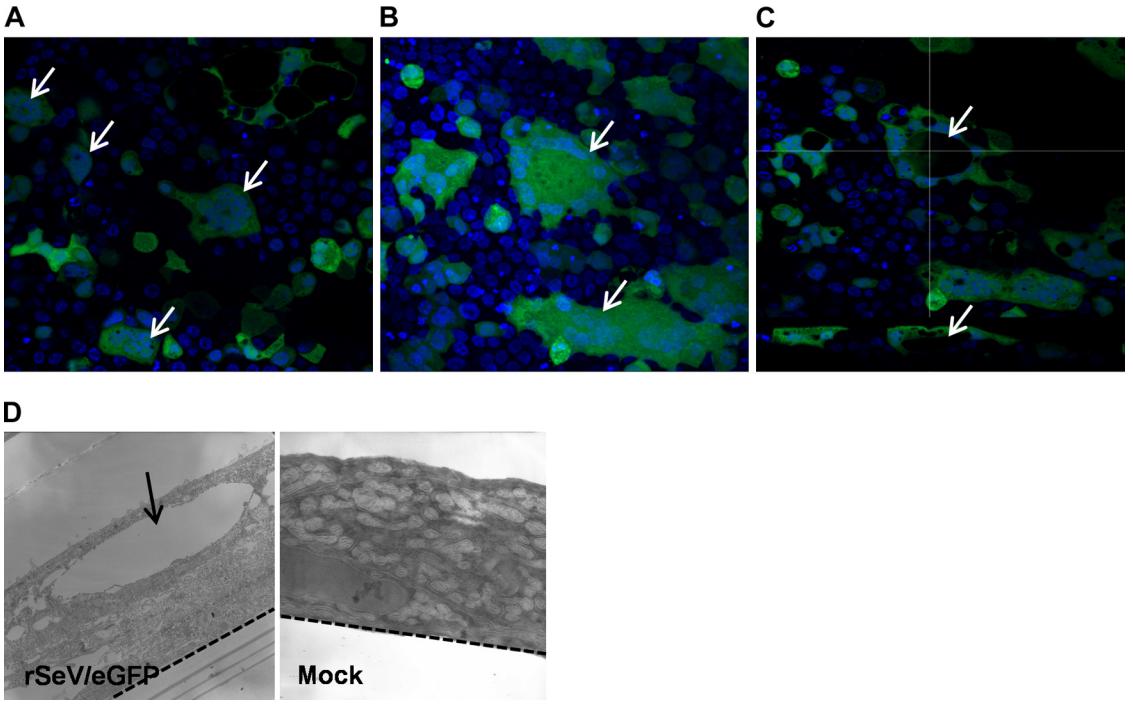

FIG. 6. rSeV/eGFP induces syncytium formation. The apical sides of WD-PBECs cultures were infected with rSeV/eGFP (MOI = 4) for 2 h and washed with PBS. At 144 hpi, WD-PBECs cultures were fixed and stained with DAPI to visualize nuclei and examined under confocal and electron microscopy. Syncytia following SeV/eGFP infection are indicated by white arrows. (A) *En face* confocal micrograph. Nuclei are clustered in the center. (B) *En face* confocal micrograph. Nuclei organized in the perimeter of the syncytia due to vacuole formation inside the syncytia. (C) Confocal *en face* view (top) and corresponding orthogonal section (bottom). The vacuole is indicated by white arrows. Original magnification, ×40. (D) Transmission electron micrographs of rSeV/eGFP (MOI = 4)- and mock-infected WD-PBEC cultures at 120 hpi. The vacuole is indicated by a black arrow, and the semipermeable basal membrane is indicated by the dashed line. Original magnification, ×15,500.

tures (mean of >30 ng/ml at 24 hpi and >140 ng/ml at 120 hpi), while those for RANTES and TRAIL were moderate. VEGF was also highly expressed but to similar levels in rSeV/eGFP- and mock-infected cultures.

DISCUSSION

SeV has a number of biological characteristics that make it particularly interesting as a vector, not least of which is its tropism for the respiratory epithelium. However, while recent preclinical studies have confirmed its potential as a vaccine vector (18), gene therapy studies using replication-incompetent SeV expressing the *cftr* gene have been less promising, primarily because of the transient nature of the transgene expression (16). Surprisingly, little is known about the interaction between SeV and the human airway epithelium, its primary target. Such knowledge is critical to help us understand the successes and failures of previous studies and improve vector efficiency.

In this study, our WD-PBEC cultures were found to have many physiologically authentic characteristics and thereby represent a relevant model system in which to study SeV/human pediatric respiratory tract interactions. We found that rSeV/eGFP efficiently infected WD-PBECs and replicated to high titers. This is consistent with previous reports of either differentiated adult human airway epithelial cells (HAE) or adult nasal epithelial cells cultured in monolayers (30, 43). Interestingly, the rSeV/eGFP growth kinetics reported here were also similar to recent results for hPIV1 infection of HAE (3). Furthermore, the restriction of rSeV/eGFP infection to apical-layer ciliated and nonciliated epithelial cells, but not goblet cells, is consistent with data derived from infection of HAE with RSV, hPIV1, hPIV3, and influenza virus (3, 4, 45, 46). In contrast, SeV infected both ciliated epithelium and secretory cells in rat tracheas following infection *in vivo* (24).

The release of progeny rSeV/eGFP exclusively from the apical surface provides strong evidence of polarized virion budding, the mechanisms of which remain to be determined. It is also consistent with previous reports of SeV, hPIV1, hPIV3, RSV, and human and avian influenza virus infections of HAE (4, 30, 37, 45, 46). Thus, apical release appears to be a general phenomenon for these common respiratory viruses. Furthermore, our data confirmed that the released rSeV/eGFP was infectious, by virtue of virus titrations being undertaken in the absence of acetylated trypsin. Its close relative hPIV1 was similarly found to be infectious following release from HAE cultures (3). Proteolytic cleavage of the SeV F_0 protein to F_1 and F_2 is essential for infectivity. In rodent lungs, this is achieved by tryptase Clara secreted from Clara cells, while *in vitro* propagation of SeV in LLC-MK2 cells requires the addition of acetylated trypsin to the tissue culture medium (17, 35). Therefore, WD-PBEC cultures clearly express a protease(s) capable of appropriate cleavage of SeV F_0. Using a Clara cell-specific polyclonal antibody, we found no evidence of Clara cells in WD-PBECs (data not shown), suggesting that

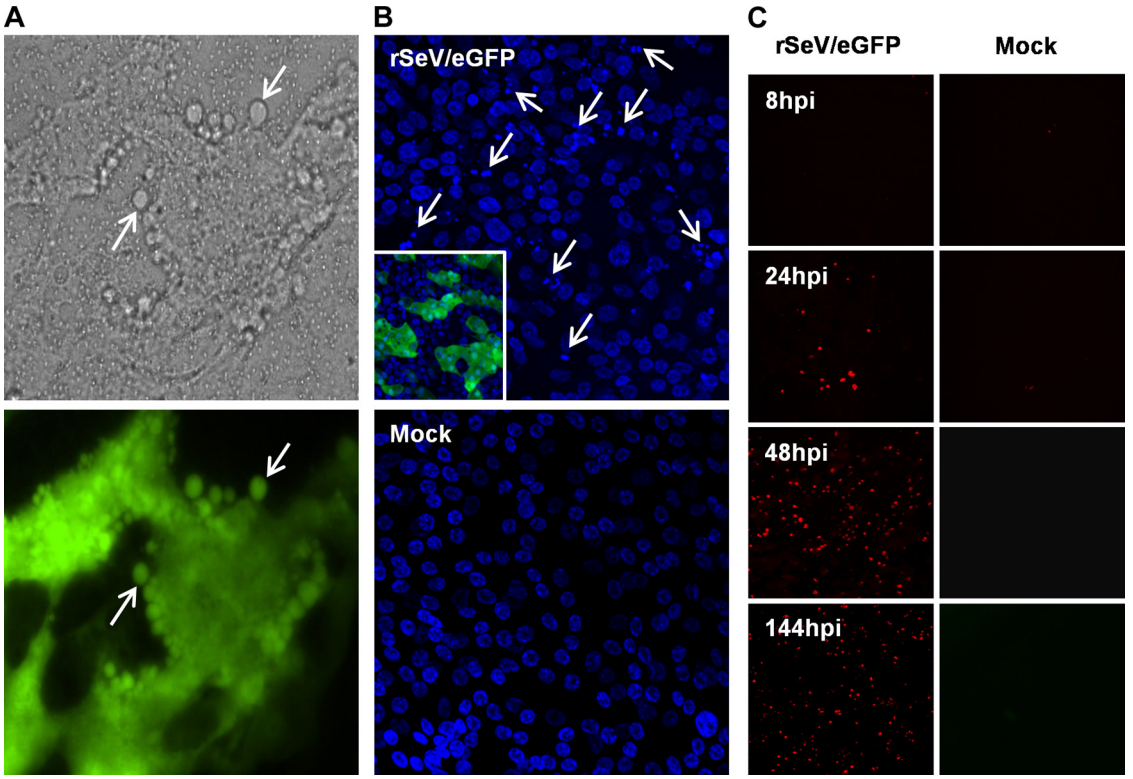

FIG. 7. rSeV/eGFP infection induces apoptosis. WD-PBECs were infected for 2 h with rSeV/eGFP (MOI = 4) and washed with PBS. (A) At 48 hpi, live WD-PBECs were monitored using a phase-contrast/UV microscope. rSeV/eGFP-infected cells appear in green. White arrows indicate apoptotic bodies. Original magnification, ×40. (B) At 144 hpi, cultures were fixed and stained with DAPI to visualize nuclei. White arrows indicate typical apoptosis-associated nuclear fragmentation and chromatin condensation. Original magnification, ×40. (C) rSeV/eGFP- and mock-infected WD-PBECs were stained in a TUNEL assay to detect cells undergoing apoptosis at 8, 24, 48, and 144 hpi. Red staining is indicative of DNA strand breaking and apoptosis. Original magnification, ×40.

other cells are responsible for expressing the necessary protease(s). Interestingly, Böttcher et al. recently identified two airway-associated proteases that efficiently cleaved the influenza virus HA0 protein (6). This suggests the possibility of more than one protease capable of cleaving SeV F_0.

Surprisingly, and in contrast to the work of Pinkenburg et al. (30), rSeV/eGFP induced substantial CPE in our WD-PBEC cultures. These results also contrast with results with hPIV1-infected HAE cultures, in which there was little gross cytopathology (3). As SeV is not known to be pathogenic to humans, this result was quite unexpected but repeated several times. The early CPE bore many hallmarks of the induction of apoptosis, as demonstrated by cell blebbing, chromatin condensation, and positive TUNEL staining. At later time points, substantially more cell sloughing was evident than in uninfected controls, as evidenced by the cytospin data. This was associated with the development of large holes in the cultures. Furthermore, epithelial culture thickness of SeV-infected cultures was often less than those of uninfected controls at late time points postinfection, indicating SeV-induced destruction of the cultures. In a novel observation, syncytium formation was commonly observed in rSeV/eGFP-infected WD-PBECs. The relatively high frequency of syncytia in SeV-infected WD-PBECs compared to their relative paucity following *in vivo* infection in mice infected with SeV or in human autopsy lung tissues from hPIV- or RSV-infected individuals (14, 21, 36) may be reconciled by the sloughing and elimination of syncytia *in vivo*, such that they are only rarely visible in tissue sections. Importantly, although a replication-competent virus was used in our study, the considerable induction of apoptosis and cell sloughing might help explain the transient nature of transgene expression in the lungs of a mouse in a murine model of CF, in which, as with our construct, SeV Z provided the backbone of the vector (14).

The discrepancies between our data and those of Pinkenburg et al. (30) in terms of culture integrity following SeV infection remain to be explained. It is possible that the origin of the epithelial cells (child versus adult), the strain of SeV used (Z versus Fushimi), and/or the location of *gfp* gene insertion within the SeV genome (between *N* and *P* versus *P* and *M*) might be implicated. Interestingly, differential CPE were recently described following infection of several different cell lines with either SeV Z or Fushimi strains, although in these monolayer cells, the latter strain was found to be the most cytopathogenic (42). As SeV is considered nonpathogenic in humans but HPIV1 is highly pathogenic, it was counterintuitive to observe substantial CPE in our rSeV/eGFP-infected cultures, while HPIV1 induced little or no CPE in HAE cultures (3). Indeed, an interesting parallel was reported for influenza A viruses, in which influenza virus A/Udorn/307/72, which induced mild febrile or upper respiratory tract symptoms in human volunteers (26), rapidly obliterated HAE cultures,

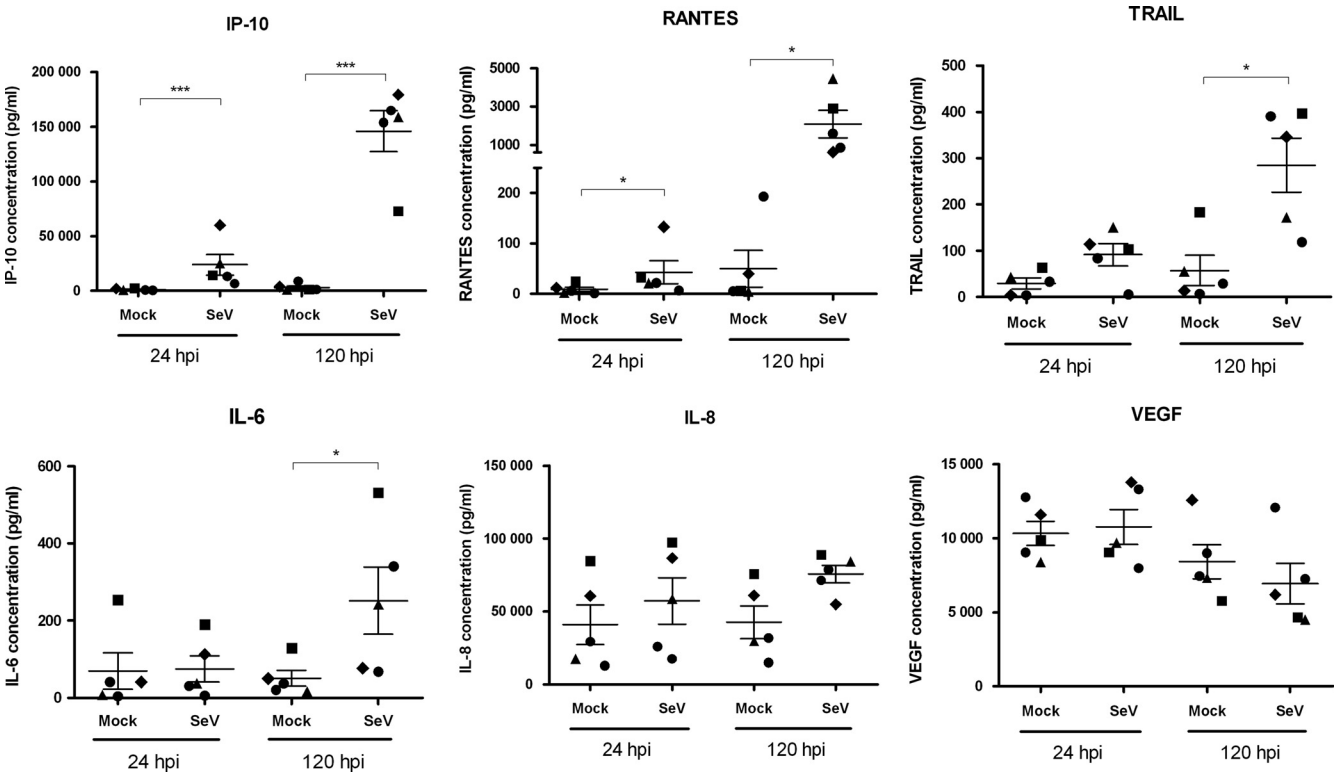

FIG. 8. Chemokine secretions induced following rSeV/eGFP infection. WD-PBECs were infected for 2 h with rSeV/eGFP (MOI = 4) and washed with PBS. Basolateral media from rSeV/eGFP and mock-infected cultures were harvested daily, stored at −80°C until used, and replaced with fresh medium. For these studies, samples harvested at 24 h and 120 h were used to determine secreted chemokine concentrations using a custom-made Bio-Plex kit. Therefore, data presented correspond to chemokine secretions within the 24-h period prior to harvesting. Each of the 5 individual donors is represented by a specific symbol that is retained for each time point and each experimental condition. Error bars correspond to standard errors. Data were analyzed using a paired *t* test. *, $P < 0.05$; ***, $P < 0.001$ for rSeV/eGFP versus mock-infected WD-PBECs.

while influenza virus H5N1 (A/VN/1203/04), which was derived from a fatal human case of avian influenza, induced no, or very limited, CPE in these cultures (32, 46). The combined data from all of these viruses suggest that virus-induced damage to HAE cultures appears to be inversely correlated with viral pathogenesis in humans. This is consistent with the work of Itoh et al., who demonstrated that a mutant SeV strain that efficiently induced apoptosis *in vitro* and *in vivo* was highly attenuated in mice compared to the virulence of its wild-type counterpart (19). Antiapoptotic activity was mapped to amino acid residues 10 to 15 of the SeV C protein (15). Furthermore, in contrast to wild-type hPIV1, a hPIV1 mutant that does not express any C proteins induced extensive CPE and apoptosis in monolayer cells and was highly growth attenuated in African green monkeys (3).

The kinetics of rSeV/eGFP growth in WD-PBECs demonstrated a highly reproducible, efficient, and productive infection in these cells (Fig. 3). The data indicate that innate antiviral responses induced following infection were insufficient to block replication and/or that rSeV/eGFP was capable of blocking at least some of these responses. The latter explanation is consistent with the work of Bousse et al., who demonstrated that SeV C proteins blocked transport of STAT1 and STAT2 to the nuclei of human monolayer cells, thereby preventing type I interferon (IFN) signaling (7). Furthermore, Kato et al. demonstrated that the hPIV1 C protein amino acid residues 151, 153, and 154, which are conserved in the SeV C protein homologue, were important for this function (23). Indeed, this provides a molecular explanation for the capacity of rSeV/eGFP to replicate efficiently in WD-PBECs. The SeV and hPIV1 C proteins have also been implicated in blocking apoptosis in a species-specific manner, and as indicated above, the domain responsible is located in the N terminus and independent of the anti-IFN signaling domains (15). Evidently, and consistent with recent reports of monolayer systems (29), our data clearly indicated that rSeV/eGFP is not capable of blocking apoptosis in WD-PBECs.

The design and exploitation of viruses as vaccine or gene therapy vectors are in many ways conceptually opposed. For vaccine vectors, the goal is to facilitate the induction of robust immune responses to the vaccine antigen, while for gene therapy vectors, limiting or circumventing such responses is key to transgene persistence. In our WD-PBEC model, rSeV/eGFP induced high levels of proinflammatory cytokines/chemokines, such as IP-10, TRAIL, RANTES, IL-6, and, to a lesser extent, IL-8 (Fig. 8). These changes are consistent with robust inflammatory responses induced following rSeV/eGFP infection. If these inflammatory responses are considered appropriate for normal host defense, our data would support the use of SeV as a vaccine vector in its current form, although not as a gene therapy vector. Alternatively, if the responses are considered overexuberant, lung pathology is the likely outcome. As SeV is

not known to be pathogenic in humans, the observed inflammatory responses are likely to be part of a normal host defense against SeV infection.

The significant upregulation of IP-10, RANTES, and IL-6 expression in rSeV/eGFP-infected WD-PBECs is of particular interest from a vaccine viewpoint, as each is under investigation as a molecular adjuvant for a variety of vaccine antigens (20, 28). Although the biological significance remains to be determined, the high levels of IL-8 secreted from mock-infected WD-PBEC cultures in our model is noteworthy and consistent with the results of previous reports (25, 39). While not significantly upregulated in rSeV/eGFP-infected cultures, the strong trend toward increased expression at 120 hpi suggests a potential role for IL-8 in anti-rSeV/eGFP immune responses.

TRAIL occurs in membrane-anchored and soluble forms (10). Both forms are potent inducers of apoptosis. The moderate levels of soluble TRAIL released from rSeV/eGFP-infected cultures, particularly at 120 hpi, are consistent with the extensive apoptosis observed. These data suggest that TRAIL might be implicated in the WD-PBEC degeneration following infection. This is also of interest from a vaccine viewpoint, as apoptotic cells are efficiently exploited by antigen-presenting cells, such as dendritic cells, to capture viral antigens and present them to cytotoxic T cells (1).

In conclusion, our data demonstrated that SeV induces robust inflammatory responses and extensive CPE in pediatric WD-PBEC cultures. This may explain, in part at least, the transient nature of transgene expression in SeV-transduced cells *in vitro* and *in vivo*. Exploitation of SeV as a gene therapy vector, therefore, is likely to require the generation of a recombinant SeV capable of persistent infection. Alternatively, the observed inflammatory and apoptotic consequences of rSeV/eGFP infection may constitute normal host responses that are necessary for the induction of robust immunity. In this case, our data would support the use of replication-competent SeV as a vaccine vector in humans. However, because the factors that control the balance between normal and overexuberant/pathogenic inflammatory responses in the lungs are unclear, prudence is prescribed for the use of replication-competent SeV as a vaccine vector, especially in infants that are immunologically naïve to hPIV1.

ACKNOWLEDGMENTS

This work was supported by Queen's University Belfast (grant to U.F.P.), the European Social Fund (grant to U.F.P.), and Northern Ireland HSC R&D of the Public Health Agency (grant RRG 9.44 to U.F.P., M.D.S., L.G.H., and G.S.).

We are most grateful to the children and parents who consented to participate in this study. Barney O'Loughlin provided excellent technical assistance.

We declare no conflicts of interest.

REFERENCES

1. **Albert, M. L., B. Sauter, and N. Bhardwaj.** 1998. Dendritic cells acquire antigen from apoptotic cells and induce class I-restricted CTLs. Nature **392:**86–89.
2. **Ban, H., M. Inoue, U. Griesenbach, F. Munkonge, M. Chan, A. Iida, E. W. Alton, and M. Hasegawa.** 2007. Expression and maturation of Sendai virus vector-derived CFTR protein: functional and biochemical evidence using a GFP-CFTR fusion protein. Gene Ther. **14:**1688–1694.
3. **Bartlett, E. J., A. M. Cruz, J. Esker, A. Castano, H. Schomacker, S. R. Surman, M. Hennessey, J. Boonyaratanakornkit, R. J. Pickles, P. L. Collins, B. R. Murphy, and A. C. Schmidt.** 2008. Human parainfluenza virus type 1 C proteins are nonessential proteins that inhibit the host interferon and apoptotic responses and are required for efficient replication in nonhuman primates. J. Virol. **82:**8965–8977.
4. **Bartlett, E. J., M. Hennessey, M. H. Skiadopoulos, A. C. Schmidt, P. L. Collins, B. R. Murphy, and R. J. Pickles.** 2008. Role of interferon in the replication of human parainfluenza virus type 1 wild-type and mutant viruses in human ciliated airway epithelium. J. Virol. **82:**8059–8070.
5. **Bitzer, M., G. Ungerechts, S. Bossow, F. Graepler, R. Sedlmeier, S. Armeanu, C. Bernloehr, M. Spiegel, C. D. Gross, M. Gregor, W. J. Neubert, and U. M. Lauer.** 2003. Negative-strand RNA viral vectors: intravenous application of Sendai virus vectors for the systemic delivery of therapeutic genes. Mol. Ther. **7:**210–217.
6. **Böttcher, E., T. Matrosovich, M. Beyerle, H. D. Klenk, W. Garten, and M. Matrosovich.** 2006. Proteolytic activation of influenza viruses by serine proteases TMPRSS2 and HAT from human airway epithelium. J. Virol. **80:** 9896–9898.
7. **Bousse, T., R. L. Chambers, R. A. Scroggs, A. Portner, and T. Takimoto.** 2006. Human parainfluenza virus type 1 but not Sendai virus replicates in human respiratory cells despite IFN treatment. Virus Res. **121:**23–32.
8. **Bukreyev, A., M. H. Skiadopoulos, B. R. Murphy, and P. L. Collins.** 2006. Nonsegmented negative-strand viruses as vaccine vectors. J. Virol. **80:**10293–10306.
9. **Conzelmann, K. K.** 2004. Reverse genetics of mononegavirales. Curr. Top. Microbiol. Immunol. **283:**1–41.
10. **Corazza, N., D. Kassahn, S. Jakob, A. Badmann, and T. Brunner.** 2009. TRAIL-induced apoptosis: between tumor therapy and immunopathology. Ann. N. Y. Acad. Sci. **1171:**50–58.
11. **Coyle, P. V., G. M. Ong, H. J. O'Neill, C. McCaughey, D. De Ornellas, F. Mitchell, S. J. Mitchell, S. A. Feeney, D. E. Wyatt, M. Forde, and J. Stockton.** 2004. A touchdown nucleic acid amplification protocol as an alternative to culture backup for immunofluorescence in the routine diagnosis of acute viral respiratory tract infections. BMC Microbiol. **4:**41.
12. **Doherty, G. M., S. N. Christie, G. Skibinski, S. M. Puddicombe, T. J. Warke, F. de Courcey, A. L. Cross, J. D. Lyons, M. Ennis, M. D. Shields, and L. G. Heaney.** 2003. Non-bronchoscopic sampling and culture of bronchial epithelial cells in children. Clin. Exp. Allergy **33:**1221–1225.
13. **Ferrari, S., U. Griesenbach, A. Iida, R. Farley, A. M. Wright, J. Zhu, F. M. Munkonge, S. N. Smith, J. You, H. Ban, M. Inoue, M. Chan, C. Singh, B. Verdon, B. E. Argent, B. Wainwright, P. K. Jeffery, D. M. Geddes, D. J. Porteous, S. C. Hyde, M. A. Gray, M. Hasegawa, and E. W. Alton.** 2007. Sendai virus-mediated CFTR gene transfer to the airway epithelium. Gene Ther. **14:**1371–1379.
14. **Ferrari, S., U. Griesenbach, T. Shiraki-Iida, T. Shu, T. Hironaka, X. Hou, J. Williams, J. Zhu, P. K. Jeffery, D. M. Geddes, M. Hasegawa, and E. W. Alton.** 2004. A defective nontransmissible recombinant Sendai virus mediates efficient gene transfer to airway epithelium in vivo. Gene Ther. **11:**1659–1664.
15. **Garcin, D., J. Curran, M. Itoh, and D. Kolakofsky.** 2001. Longer and shorter forms of Sendai virus C proteins play different roles in modulating the cellular antiviral response. J. Virol. **75:**6800–6807.
16. **Griesenbach, U., E. W. Alton, and UK Cystic Fibrosis Gene Therapy Consortium.** 2009. Gene transfer to the lung: lessons learned from more than 2 decades of CF gene therapy. Adv. Drug Deliv. Rev. **61:**128–139.
17. **Homma, M.** 1971. Trypsin action on the growth of Sendai virus in tissue culture cells. I. Restoration of the infectivity for L cells by direct action of trypsin on L cell-borne Sendai virus. J. Virol. **8:**619–629.
18. **Hurwitz, J. L., K. F. Soike, M. Y. Sangster, A. Portner, R. E. Sealy, D. H. Dawson, and C. Coleclough.** 1997. Intranasal Sendai virus vaccine protects African green monkeys from infection with human parainfluenza virus-type one. Vaccine **15:**533–540.
19. **Itoh, M., H. Hotta, and M. Homma.** 1998. Increased induction of apoptosis by a Sendai virus mutant is associated with attenuation of mouse pathogenicity. J. Virol. **72:**2927–2934.
20. **Jiang, X. B., X. L. Lu, P. Hu, and R. E. Liu.** 2009. Improved therapeutic efficacy using vaccination with glioma lysate-pulsed dendritic cells combined with IP-10 in murine glioma. Vaccine **24:**6210–6216.
21. **Johnson, J. E., R. A. Gonzales, S. J. Olson, P. F. Wright, and B. S. Graham.** 2007. The histopathology of fatal untreated human respiratory syncytial virus infection. Mod. Pathol. **20:**108–119.
22. **Jones, B., X. Zhan, V. Mishin, K. S. Slobod, S. Surman, C. J. Russell, A. Portner, and J. L. Hurwitz.** 2009. Human PIV-2 recombinant Sendai virus (rSeV) elicits durable immunity and combines with two additional rSeVs to protect against hPIV-1, hPIV-2, hPIV-3, and RSV. Vaccine **27:**1848–1857.
23. **Kato, A., C. Cortese-Grogan, S. A. Moyer, F. Sugahara, T. Sakaguchi, T. Kubota, N. Otsuki, M. Kohase, M. Tashiro, and Y. Nagai.** 2004. Characterization of the amino acid residues of Sendai virus C protein that are critically involved in its interferon antagonism and RNA synthesis down-regulation. J. Virol. **78:**7443–7454.
24. **Massion, P. P., C. C. Funari, I. Ueki, S. Ikeda, D. M. McDonald, and J. A. Nadel.** 1993. Parainfluenza (Sendai) virus infects ciliated cells and secretory cells but not basal cells of rat tracheal epithelium. Am. J. Respir. Cell Mol. Biol. **9:**361–370.

25. **Mellow, T. E., P. C. Murphy, J. L. Carson, T. L. Noah, L. Zhang, and R. J. Pickles.** 2004. The effect of respiratory syncytial virus on chemokine release by differentiated airway epithelium. Exp. Lung Res. **30:**43–57.
26. **Murphy, B. R., D. L. Sly, N. T. Hosier, W. T. London, and R. M. Chanock.** 1980. Evaluation of three strains of influenza A virus in humans and in owl, cebus, and squirrel monkeys. Infect. Immun. **28:**688–691.
27. **Parker, J., S. Sarlang, S. Thavagnanam, G. Williamson, D. O'donoghue, R. Villenave, U. Power, M. Shields, L. Heaney, and G. Skibinski.** 2010. A 3-D well-differentiated model of pediatric bronchial epithelium demonstrates un-stimulated morphological differences between asthmatic and non-asthmatic cells. Pediatr. Res. **67:**17–22.
28. **Pertl, U., A. D. Luster, N. M. Varki, D. Homann, G. Gaedicke, R. A. Reisfeld, and H. N. Lode.** 2001. IFN-gamma-inducible protein-10 is essential for the generation of a protective tumor-specific CD8 T cell response induced by single-chain IL-12 gene therapy. J. Immunol. **166:**6944–6951.
29. **Peters, K., S. Chattopadhyay, and G. C. Sen.** 2008. IRF-3 activation by Sendai virus infection is required for cellular apoptosis and avoidance of persistence. J. Virol. **82:**3500–3508.
30. **Pinkenburg, O., C. Vogelmeier, S. Bossow, W. J. Neubert, R. B. Lutz, G. Ungerechts, U. M. Lauer, M. Bitzer, and R. Bals.** 2004. Recombinant Sendai virus for efficient gene transfer to human airway epithelium. Exp. Lung Res. **30:**83–96.
31. **Scheid, A., and P. W. Choppin.** 1974. Identification of biological activities of paramyxovirus glycoproteins. Activation of cell fusion, hemolysis, and infectivity of proteolytic cleavage of an inactive precursor protein of Sendai virus. Virology **57:**475–490.
32. **Scull, M. A., L. Gillim-Ross, C. Santos, K. L. Roberts, E. Bordonali, K. Subbarao, W. S. Barclay, and R. J. Pickles.** 2009. Avian Influenza virus glycoproteins restrict virus replication and spread through human airway epithelium at temperatures of the proximal airways. PLoS Pathog. **5:**e1000424.
33. **Slobod, K. S., J. L. Shenep, J. Lujan-Zilbermann, K. Allison, B. Brown, R. A. Scroggs, A. Portner, C. Coleclough, and J. L. Hurwitz.** 2004. Safety and immunogenicity of intranasal murine parainfluenza virus type 1 (Sendai virus) in healthy human adults. Vaccine **22:**3182–3186.
34. **Takimoto, T., J. L. Hurwitz, X. Zhan, S. Krishnamurthy, C. Prouser, B. Brown, C. Coleclough, K. Boyd, R. A. Scroggs, A. Portner, and K. S. Slobod.** 2005. Recombinant Sendai virus as a novel vaccine candidate for respiratory syncytial virus. Viral Immunol. **18:**255–266.
35. **Tashiro, M., Y. Yokogoshi, K. Tobita, J. T. Seto, R. Rott, and H. Kido.** 1992. Tryptase Clara, an activating protease for Sendai virus in rat lungs, is involved in pneumopathogenicity. J. Virol. **66:**7211–7216.
36. **Terrier, O., G. Cartet, O. Ferraris, F. Morfin, D. Thouvenot, S. S. Hong, and B. Lina.** 2008. Characterization of naturally occurring parainfluenza virus type 2 (hPIV-2) variants. J. Clin. Virol. **43:**86–92.
37. **Thompson, C. I., W. S. Barclay, M. C. Zambon, and R. J. Pickles.** 2006. Infection of human airway epithelium by human and avian strains of influenza a virus. J. Virol. **80:**8060–8068.
38. **Touzelet, O., N. Loukili, T. Pelet, D. Fairley, J. Curran, and U. F. Power.** 2009. De novo generation of a non-segmented negative strand RNA virus with a bicistronic gene. Virus Res. **140:**40–48.
39. **Tristram, D. A., W. Hicks, Jr., and R. Hard.** 1998. Respiratory syncytial virus and human bronchial epithelium. Arch. Otolaryngol. Head Neck Surg. **124:**777–783.
40. **Tsukamoto, T., A. Takeda, T. Yamamoto, H. Yamamoto, M. Kawada, and T. Matano.** 2009. Impact of cytotoxic-T-lymphocyte memory induction without virus-specific $CD4^+$ T-cell help on control of a simian immunodeficiency virus challenge in rhesus macaques. J. Virol. **83:**9339–9346.
41. **Voges, B., S. Vallbracht, G. Zimmer, S. Bossow, W. J. Neubert, K. Richter, E. Hobeika, G. Herrler, and S. Ehl.** 2007. Recombinant Sendai virus induces T cell immunity against respiratory syncytial virus that is protective in the absence of antibodies. Cell. Immunol. **247:**85–94.
42. **Wiegand, M., S. Bossow, and W. J. Neubert.** 2005. Sendai virus trailer RNA simultaneously blocks two apoptosis-inducing mechanisms in a cell type-dependent manner. J. Gen. Virol. **86:**2305–2314.
43. **Yonemitsu, Y., C. Kitson, S. Ferrari, R. Farley, U. Griesenbach, D. Judd, R. Steel, P. Scheid, J. Zhu, P. K. Jeffery, A. Kato, M. K. Hasan, Y. Nagai, I. Masaki, M. Fukumura, M. Hasegawa, D. M. Geddes, and E. W. Alton.** 2000. Efficient gene transfer to airway epithelium using recombinant Sendai virus. Nat. Biotechnol. **18:**970–973.
44. **Zhan, X., J. L. Hurwitz, S. Krishnamurthy, T. Takimoto, K. Boyd, R. A. Scroggs, S. Surman, A. Portner, and K. S. Slobod.** 2007. Respiratory syncytial virus (RSV) fusion protein expressed by recombinant Sendai virus elicits B-cell and T-cell responses in cotton rats and confers protection against RSV subtypes A and B. Vaccine **25:**8782–8793.
45. **Zhang, L., A. Bukreyev, C. I. Thompson, B. Watson, M. E. Peeples, P. L. Collins, and R. J. Pickles.** 2005. Infection of ciliated cells by human parainfluenza virus type 3 in an in vitro model of human airway epithelium. J. Virol. **79:**1113–1124.
46. **Zhang, L., M. E. Peeples, R. C. Boucher, P. L. Collins, and R. J. Pickles.** 2002. Respiratory syncytial virus infection of human airway epithelial cells is polarized, specific to ciliated cells, and without obvious cytopathology. J. Virol. **76:**5654–5666.